Conceptual DFT analysis of the fragility spectra of atoms along the minimum energy reaction coordinate

Piotr Ordon, Ludwik Komorowski, and Mateusz Jedrzejewski

Citation: The Journal of Chemical Physics **147**, 134109 (2017); doi: 10.1063/1.4995028
View online: http://dx.doi.org/10.1063/1.4995028
View Table of Contents: http://aip.scitation.org/toc/jcp/147/13
Published by the American Institute of Physics

Conceptual DFT analysis of the fragility spectra of atoms along the minimum energy reaction coordinate

Piotr Ordon,[1,a)] Ludwik Komorowski,[2] and Mateusz Jędrzejewski[2]
[1]*Department of Physics and Biophysics, Wrocław University of Environmental and Life Sciences, ul. Norwida 25, 50-375 Wrocław, Poland*
[2]*Department of Physical and Quantum Chemistry, Wrocław University of Science and Technology, Wyb. Wyspiańskiego 27, 50-370 Wrocław, Poland*

(Received 10 July 2017; accepted 11 September 2017; published online 4 October 2017)

Theoretical justification has been provided to the method for monitoring the sequence of chemical bonds' rearrangement along a reaction path, by tracing the evolution of the diagonal elements of the Hessian matrix. Relations between the divergences of Hellman-Feynman forces and the energy and electron density derivatives have been demonstrated. By the proof presented on the grounds of the conceptual density functional theory formalism, the spectral amplitude observed on the atomic fragility spectra [L. Komorowski *et al.*, Phys. Chem. Chem. Phys. **18**, 32658 (2016)] reflects selectively the electron density modifications in bonds of an atom. In fact the spectral peaks for an atom reveal changes of the electron density occurring with bonds creation, breaking, or varying with the reaction progress. *Published by AIP Publishing.* https://doi.org/10.1063/1.4995028

I. INTRODUCTION

The theory of electronic reorganization in chemical entities (atoms and molecules) has been an important goal of the conceptual density functional theory (cDFT) whose development has been parallel to the progress in the computational techniques for nearly 40 years[1,2] since the landmark papers by Parr *et al.*[3] and Parr and Pearson.[4] The comprehensive review of conceptual DFT has been provided by Chermette[5] and by Geerlings *et al.*[6,7] Exploring the achievements of cDFT within the framework of the computational analysis of a reaction dynamics presents a challenging task in describing the evolution of the electron density $\rho(\mathbf{r})$ function when the reaction is in progress.[8] Resolution of the involved interplay between electronic and geometric degrees of freedom has been subject to the fundamental work by Nalewajski.[9]

The key to the cDFT analysis of the electronic structure properties are the electronic energy derivatives; they have long been recognized as potential site reactivity indicators.[10,11] Parr and Nalewajski first formulated a systematic approach to the whole set of derivatives of energy as an electron-density functional.[12–14] They defined Legendre transforms of the energy functional for the system within various constraints and derived a variety of Maxwell-type phenomenological cross relations between functional derivatives. This approach enabled the formulation of sensitivity analysis, identifying local and global linear-response functions to some external perturbation.[15–20] Ayers and Parr[21] continued this approach and studied the energy derivatives as functions of an appropriate set of parameters. Ayers *et al.*[22] have chosen to analyze the energy derivatives up to the third order, both in canonical and grand canonical ensembles, which were appropriately renamed for closed and open systems, respectively. Relationships between many energy derivatives have been either confirmed or newly demonstrated in this study. In their analysis, the external potential function $\upsilon(\mathbf{r})$ served as an independent variable for the energy functional and was combined with the number of electrons (N) for a closed system and with the chemical potential of electrons $\mu = (\partial E/\partial N)_{\upsilon(\mathbf{r})}$ for an open system.

An earlier theoretical work focused on this target was published by Hunt *et al.*[23–26] The response of the electronic-charge distribution to an infinitesimal shift in the position of a nucleus within the molecule had been proved to occur via the same nonlocal polarizability and hyperpolarizability densities that characterize the perturbation by an external electric field[26] and that have been later reviewed by Ayers *et al.*[22] Hunt *et al.* presented a rigorous analysis connecting nonlocal polarizability and hyperpolarizability to the intensities of Raman spectra,[25] to vibrational force constants, and to anharmonicities.[24] The authors paid particular attention to the Hellman-Feynman forces exerted on nuclei, i.e., the derivative of the electronic energy of a system over the position of a given nucleus.[27] They demonstrated that the force on a nucleus in a molecule depends on the unperturbed charge distribution of another object approaching it, including the electronic polarization induced in the host by the perturbing species.[28] This analysis provided a hint to the potential role of the Hellman-Feynman force in the analysis of the transformation of electronic structure along a reaction path.

Molecular energy derivatives over nuclear displacement in a closed system have a very well understood meaning in

a)Author to whom correspondence should be addressed: piotr.ordon@upwr.edu.pl

DFT. Their history dates back to the work by Cohen *et al.*[29] who first proposed the nuclear reactivity function (also known as the nuclear Fukui function) as a derivative of the Hellman-Feynman force at a nucleus ($\mathbf{F}_A$) over the number of electrons: $\mathbf{\Phi}_A = (\partial \mathbf{F}_A/\partial N)_\upsilon$. The concept has been explored by several authors.[30–38] The detailed review of these studies and the complete analysis of the energy derivatives over the nuclear displacement and their relations have been presented in the papers from this laboratory.[39,40] A related study demonstrated how these derivatives account for the observed anharmonic effects of molecular vibrations.[41]

A leitmotiv of the work by Ayers *et al.* and also by Hunt *et al.* was the electron-preceding perspective[42] defined as the electron density that first responds to a perturbation introduced by an external field. In the description of such an effect, the local derivatives must apply. However, the typical viewpoint in computational chemistry is the electron-following approach as a consequence of the Born–Oppenheimer approximation. The electronic structure is observed as it follows the displacement of nuclei, either by the IRC model[43] or by the arbitrary collision model along the minimum energy coordinate (MEC[44]), possibly combined with statistical theories.[45] The Hohenberg and Kohn DFT theorem is instrumental here:[46] electron density is uniquely adapted to be in equilibrium within the external potential of the nuclei at every step of a chosen trajectory and the existence of the density functional determines the chemical potential that is equalized throughout the whole reacting molecule[12] and evolving on the reaction path.[47]

Computational analysis of the energy derivatives over the reaction progress (ξ) along the reaction path has been initiated by Toro-Labbe *et al.*[48–50] By defining the reaction force ($F_\xi = -dE/d\xi$), the authors argued that the electronic rearrangement may preferentially occur in the central transition state region.[51] Ordon and Tachibana have studied reactivity index variations along an IRC to establish the most chemically reactive state.[47,52,53] Gonzalez *et al.* examined stationary conditions of the electron density along the IRC path both from reactivity indices point of view and from information theory.[54]

The Hellman-Feynman forces along the reaction path have been focused on in the earlier work by the present authors.[55] Tools have been developed for direct observation of the role of individual atoms on the system evolution from reactants to products using the Hellman-Feynman force derivatives. In the next step, the visualization method has been proposed that shows how individual bonds form, alter, or break in the course of a reaction.[56] When the derivative $(d/d\xi)$ of the trace of the system Hessian has been decomposed to atomic contributions, the picture was produced describing the variation of bonding status for an atom at every step along the reaction coordinate. The resulting two-dimensional diagram characteristic for a chosen reaction path has been called the reaction fragility spectrum. It allows for identification of the points on the reaction path where rapid changes in atomic contributions occur.

This spectrum may be a valuable result of the electronic structure calculations for practical chemistry.[57,58] In the review of the chemical dynamics simulations by Hase *et al.*,[59] the authors demonstrated how the coupled calculations of the electronic structure and the chemical dynamics have been extensively used to understand the chemical reaction at the atomic level. The dynamical techniques leading to the pathways and rates of many reactions discussed in this paper illustrate the characteristic feature of this type of research: it is focused on the potential energy surface rather than on the details of the electron density.[60] The present analysis is concentrated on the density modifications around atoms as they react.

This article is focused on the interpretation of the reaction fragility spectrum by means of the theoretical apparatus of conceptual DFT. The relevant energy derivatives in the nuclear-coordinate representation, as related to the functional derivatives, are presented first, within the new scheme of vector analysis leading to the cumulative harmonic force constants. The general relation between these derivatives and the local ones has been provided. The formal DFT interpretation of the newly defined cumulative force constants collected in the connectivity matrix has been presented. The derivatives are then applied to expose the variations of the individual atomic components to the trace of the system Hessian. Finally, quantitative factors that contribute to the intensities of atomic peaks on the reaction fragility spectrum are demonstrated.

II. ENERGY DERIVATIVES IN THE NUCLEAR COORDINATE REPRESENTATION

In a closed system, the number of electrons N is well defined and serves as a global variable. An open system is one that is free to exchange electrons with some external reservoir whose chemical potential μ is well defined and is chosen to be the global variable. It is assumed that all derivatives exist, which is the case for non-zero temperatures.[61] To bring the analysis closer to real applications, traditional names and definitions for the derivatives are used. Also, the compact notation of vector derivatives is introduced.

The appropriate state functions are the electronic energy, $E[N, \upsilon(\mathbf{r})]$, in a closed system, and the grand potential $\Omega[\mu, \upsilon(\mathbf{r})] = E - \mu N$, in an open system (exchanging electrons with a reservoir);[10] the open system and closed system representations are equivalent as pointed out by Ayers.[22] Global derivatives in both systems are $E^{(N)} = \mu$ (chemical potential), $E^{(NN)} = \eta$ (the global hardness), $\mathbf{\Omega}^{(\mu)} = -N$ (number of electrons), and $\Omega^{(\mu\mu)} = -S$ (global softness).

Both systems will be divided into equivalent representations: external potential $[\upsilon(\mathbf{r})]$ and nuclear coordinates $\{\mathbf{R}\}$. Derivatives with respect to the coordinate of a given atom $\mathbf{R}_A$ are presented by means of divergence/gradient notation rather than by commonly used derivatives over each coordinate separately (supplementary material, p. 1). Since this formulation is crucial for the final results, all derivatives up to the 3rd order have been collected for both systems.

Variational derivatives over the external potential $\upsilon(\mathbf{r})$ and the derivatives over the nuclear displacements for any physical quantity X (scalar or vector) in these two representations are bound by the general relation

$$\nabla_A \mathrm{X} = \int \frac{\delta \mathrm{X}}{\delta \upsilon(\mathbf{r})} \nabla_A \upsilon(\mathbf{r}) d\mathbf{r} = -\int \frac{\delta \mathrm{X}}{\delta \upsilon(\mathbf{r})} \boldsymbol{\varepsilon}_A(\mathbf{r}) d\mathbf{r}. \quad (1)$$

Vector $\boldsymbol{\varepsilon}_A(\mathbf{r})$ is the electrostatic field from the nucleus A; Eq. (1) holds for both systems (supplementary material, p. 2) since

$$[\nabla_A \upsilon(\mathbf{r})]_N = [\nabla_A \upsilon(\mathbf{r})]_\mu \equiv -\boldsymbol{\varepsilon}_A(\mathbf{r}). \tag{2}$$

Equation (1) will be used to translate the equations formulated in the external-potential representation (more explored theoretically) to the nuclear-coordinate representation (more suitable for experimental connections and computations). First derivatives of the electronic energy (E) are identical in both systems,

$$E^{(\upsilon)} = \rho(\mathbf{r}) \;\text{ since }\; dE = \mu dN + \int \rho(\mathbf{r})\delta\upsilon(\mathbf{r})dr, \tag{3}$$

$$\begin{aligned}\Omega^{(\upsilon)} &= \rho(\mathbf{r}) \;\text{ since }\; d\Omega = dE - \mu dN + Nd\mu \\ &= -Nd\mu + \int \rho(\mathbf{r})\delta\upsilon(\mathbf{r})dr.\end{aligned} \tag{4}$$

In the nuclear-coordinate representation, the inter-nuclear repulsion must not be neglected for the first derivative since

$$E^{(R)}_{tot} = \Omega^{(R)}_{tot} = \mathbf{F}_A + \mathbf{F}^{n-n}_A. \tag{5}$$

The Hellmann-Feynman force ($\mathbf{F}_A$) acting on a nucleus for the exact density $\rho(\mathbf{r})$ is obtained by the transformation [Eqs. (1)–(3)]

$$\mathbf{F}_A = \int \rho(\mathbf{r})\boldsymbol{\varepsilon}_A(\mathbf{r}) = -\nabla_A E = -\nabla_A \Omega. \tag{6}$$

The inter-nuclear term $\mathbf{F}^{n-n}_A$ is represented by

$$\mathbf{F}^{n-n}_A = \sum_{B\neq A}^{atoms} Z_B \boldsymbol{\varepsilon}_A(\mathbf{R}_B). \tag{7}$$

$\mathbf{F}^{n-n}_A$ is immaterial to the derivatives of force in the nuclear-coordinate representation since it is independent of N, and, also, $\nabla_A \cdot \mathbf{F}^{n-n}_A = 0$ and $\nabla_{B\neq A} \cdot \mathbf{F}^{n-n}_A = 0$ (supplementary material, p. 3).

The closed system is the basic platform for the analysis of atoms and molecules characterized by a definite number of electrons. Derivatives defined here have common names: Fukui function $E^{(\upsilon N)} = f(\mathbf{r})$ and density linear response function $E^{(\upsilon\upsilon)} = \omega(\mathbf{r},\mathbf{r})$. In the nuclear-coordinate representation, the 2nd order derivatives become

$$E^{(RN)} = -[\nabla_A \mu]_N = \left(\frac{\partial \mathbf{F}_A}{\partial N}\right)_{\{\mathbf{R}\}} \equiv \boldsymbol{\Phi}_A \qquad \text{nuclear Fukui function}^{29} \tag{8}$$

$$E^{(RR)} = [\nabla_A \cdot \mathbf{F}_B]_N \equiv \mathrm{k}_{AB} \qquad \text{cumulative harmonic force constant.} \tag{9}$$

The cumulative force constants have been defined as divergences (numbers) representing the trace (invariant) of the matrix, while the harmonic force constants are typically calculated as elements of a 3×3 matrix. The present formulation is sufficient for further analysis of the electric field derivatives and will be dealt with in detail in Sec. III.

The 3rd order cumulative derivatives in the nuclear coordinate representation in a closed system are

$$E^{(RNN)} = [\nabla_A \eta]_N = \left(\frac{\partial^2 \mathbf{F}_A}{\partial N^2}\right)_{\{\mathbf{R}\}} \equiv \mathbf{G}_A \qquad \text{nuclear stiffness vector,}^{33} \tag{10}$$

$$E^{(RRN)} = [\nabla_A \cdot \nabla_B \mu]_N \equiv \lambda_{AB} \qquad \text{softening index,}^{35,39,47} \tag{11}$$

$$E^{(RRR)} = [\nabla_C \cdot \nabla_B \cdot \mathbf{F}_A]_N \equiv \boldsymbol{\alpha}_{CBA} \qquad \text{cumulative cubic force constant vector.}^{41} \tag{12}$$

In an open system, the 2nd order derivatives in the external potential representation are local softness $\Omega^{(\upsilon\mu)} = s(\mathbf{r})$ and softness kernel $\Omega^{(\upsilon\upsilon)} = -s(\mathbf{r},\mathbf{r}')$. In the nuclear coordinate representation, the derivatives are also related to their counterparts in the closed system,

$$\Omega^{(R\mu)} = [\nabla_A N]_\mu = \left(\frac{\partial \mathbf{F}_A}{\partial \mu}\right)_{\{\mathbf{R}\}} = \boldsymbol{\Phi}_A S \qquad \text{the nuclear softness,}^{29,39} \tag{13}$$

$$\Omega^{(RR)} = [\nabla_A \cdot \mathbf{F}_B]_\mu = \widetilde{\mathrm{k}}_{AB} = \mathrm{k}_{AB} - S\boldsymbol{\Phi}_A \cdot \boldsymbol{\Phi}_B. \tag{14}$$

3rd order derivatives in the nuclear coordinate representation for an open system have been listed separately with their relation to the corresponding derivatives in the closed system (supplementary material, p. 4).

The density derivatives in both systems are especially interesting,[39,62]

$$E^{(\upsilon R)} = [\nabla_A \rho(\mathbf{r})]_N = -\int \omega(\mathbf{r},\mathbf{r}')\boldsymbol{\varepsilon}_A(\mathbf{r}')d\mathbf{r}' = \boldsymbol{\varpi}_A(\mathbf{r}), \tag{15}$$

$$\Omega^{(\upsilon R)} = [\nabla_A \rho(\mathbf{r})]_\mu = \int s(\mathbf{r},\mathbf{r}')\boldsymbol{\varepsilon}_A(\mathbf{r}')d\mathbf{r}' = \boldsymbol{\sigma}_A(\mathbf{r}). \tag{16}$$

Since the linear response function $\omega(\mathbf{r},\mathbf{r}')$ and the softness kernel $s(\mathbf{r},\mathbf{r}')$ are bound by the Parr-Berkowitz relation[63] [Eq. (17)], so are their nuclear coordinate counterparts[62] [Eq. (18)]

$$\omega(\mathbf{r},\mathbf{r}') = -s(\mathbf{r},\mathbf{r}') + s(\mathbf{r})f(\mathbf{r}'), \tag{17}$$

$$\boldsymbol{\varpi}_A(\mathbf{r}) = -s(\mathbf{r})\boldsymbol{\Phi}_A + \boldsymbol{\sigma}_A(\mathbf{r}). \tag{18}$$

The relation between the cumulative harmonic force constants in both systems [Eq. (14)] becomes the next step of this formula.

In the electron-following perspective, both quantities (vectors), $\boldsymbol{\varpi}_A(\mathbf{r})$, $\boldsymbol{\sigma}_A(\mathbf{r})$, represent the local shift of the density due to the displacement in the position of a nucleus, hence describing a property quite desirable for reactivity studies. In the electron-preceding perspective, $\boldsymbol{\varpi}_A(\mathbf{r})$ and $\boldsymbol{\sigma}_A(\mathbf{r})$ also contain information on how sensitive a chosen nucleus is to the disturbance of the density at a point at some distance $\mathbf{r}$.

III. THEORETICAL BACKGROUND

A. The connectivity matrix

The divergence $\nabla_A \cdot \mathbf{F}_B$ represents the trace of an ordinary force-constant matrix for a pair of atoms A, B,

$$\underline{\underline{K}}_{AB} = \begin{bmatrix} \frac{\partial F_{A,x}}{\partial R_{B,x}} & \frac{\partial F_{A,x}}{\partial R_{B,y}} & \frac{\partial F_{A,x}}{\partial R_{B,z}} \\ \frac{\partial F_{A,y}}{\partial R_{B,x}} & \frac{\partial F_{A,y}}{\partial R_{B,y}} & \frac{\partial F_{A,y}}{\partial R_{B,z}} \\ \frac{\partial F_{A,z}}{\partial R_{B,x}} & \frac{\partial F_{A,z}}{\partial R_{B,y}} & \frac{\partial F_{A,z}}{\partial R_{B,z}} \end{bmatrix} = \begin{bmatrix} k_{xx}^{AB} & k_{xy}^{AB} & k_{xz}^{AB} \\ k_{yx}^{AB} & k_{yy}^{AB} & k_{yz}^{AB} \\ k_{zx}^{AB} & k_{zy}^{AB} & k_{zz}^{AB} \end{bmatrix}. \tag{19}$$

The specific form of this matrix varies with the choice of the coordinate system; its invariant trace (the divergence) represents the cumulative derivative $\nabla_A \cdot \mathbf{F}_B$. The whole collection of $\underline{\underline{K}}_{AB}$ 3×3 matrices for all atoms in a system, when unified in one $3n \times 3n$ matrix, is the system Hessian. The invariants $\nabla_A \cdot \mathbf{F}_B$ themselves may be collected in the $n \times n$ connectivity matrix $\underline{\underline{C}}$ [Eq. (20)]. To underline their distinction from the elements of the Hessian, we have called them cumulative derivatives (force constants). Elements of this matrix are all invariant with respect to the rotations or shifts of the coordinate system. They characterize the particular atom-in-molecule (the diagonal elements) and contain some information on the nature of the inter-atomic contact (the off-diagonal elements),

$$\underline{\underline{C}} = \begin{bmatrix} \nabla_A \cdot \mathbf{F}_A & \nabla_A \cdot \mathbf{F}_B & \dots & \nabla_A \cdot \mathbf{F}_N \\ \nabla_B \cdot \mathbf{F}_A & \nabla_B \cdot \mathbf{F}_B & \dots & \dots \\ \dots & \dots & \dots & \dots \\ \nabla_N \cdot \mathbf{F}_A & \dots & \dots & \nabla_N \cdot \mathbf{F}_N \end{bmatrix}. \tag{20}$$

When a system loses one of its atoms (Z) by dissociation, its corresponding elements in the connectivity matrix ($\nabla_Z \cdot \mathbf{F}_Z$ and all $\nabla_{B\neq Z} \cdot \mathbf{F}_Z$) vanish since the energy will no longer depend on the position of that atom. This emphasizes that the connectivity matrix provides critical information about the deformation of a system on a reaction path.

B. Properties of the Hellman-Feynman force divergences

An important characteristic of the connectivity matrix is that its elements do not contain the contribution from internuclear interactions [Eq. (7)]. This makes them a convenient medium to trace the evolution of the electronic structure along a chosen minimum-energy reaction coordinate.[44] The Hellman-Feynman force acting on a nucleus is bound to the electron-density function by the simple relation [Eq. (6)]. The elements of the connectivity matrix [Eq. (20)] are found by its appropriate differentiation. By using electrodynamical relations (supplementary material, p. 2), the results are reduced to

$$[\nabla_A \cdot \mathbf{F}_A]_N = 4\pi Z_A \rho(\mathbf{R}_A) + \int \boldsymbol{\varepsilon}_A(\mathbf{r}) \cdot [\nabla_A \rho(\mathbf{r})]_N d\mathbf{r}, \tag{21}$$

$$[\nabla_{B\neq A} \cdot \mathbf{F}_A]_N = \int \boldsymbol{\varepsilon}_A(\mathbf{r}) \cdot [\nabla_{B\neq A} \rho(\mathbf{r})]_N d\mathbf{r}. \tag{22}$$

This is equivalent to the formula expressed by Hunt *et al.* in the language of the dipole propagator[24] and to the ones in earlier studies by Salem *et al.*[64–66] The results in Eqs. (21) and (22) may be presented in compact form in the DFT language [Eq. (15)], and by introducing the Kronecker delta δ_{BA},

$$[\nabla_A \cdot \mathbf{F}_B]_N = 4\pi Z_A \rho(\mathbf{R}_A)\delta_{BA} - \iint \omega(\mathbf{r},\mathbf{r}')\boldsymbol{\varepsilon}_A(\mathbf{r}') \cdot \boldsymbol{\varepsilon}_B(\mathbf{r}) d\mathbf{r}' d\mathbf{r}. \tag{23}$$

Equation (23) is exact in reproducing the property of the newly formulated cumulative second derivatives of the energy (divergences of forces). It may be transformed with the Parr-Berkowitz equation [Eq. (17)] to an equivalent form that will eventually be explored,

$$[\nabla_A \cdot \mathbf{F}_B]_N = 4\pi Z_A \rho(\mathbf{R}_A)\delta_{BA} - S\boldsymbol{\Phi}_A \cdot \boldsymbol{\Phi}_B + \iint s(\mathbf{r},\mathbf{r}')\boldsymbol{\varepsilon}_A(\mathbf{r}') \cdot \boldsymbol{\varepsilon}_B(\mathbf{r}) d\mathbf{r} d\mathbf{r}'. \tag{24}$$

The divergence formulation of the derivatives leads to exact formulae for describing properties of the electron density. The sum of forces over all atoms vanishes [Eq. (5)],

$$\sum_B \left(\mathbf{F}_B + \mathbf{F}_B^{n-n}\right) = 0. \tag{25}$$

Since the divergence of all nuclear forces is zero (supplementary material, p. 3), the sum of divergences for $\nabla_A \cdot \sum_B \mathbf{F}_B$ must also be zero. Hence, the following property of the connectivity matrix is proved:

$$[\nabla_A \cdot \mathbf{F}_A]_N = -\sum_B^{atoms} [\nabla_A \cdot \mathbf{F}_{B\neq A}]_N. \tag{26}$$

C. Reaction fragility for a reacting atom

The reaction fragility spectrum for an atom in molecule a_ξ^A has been defined as the computed derivative,[56]

$$a_\xi^A = \frac{d}{d\xi}(\nabla_A \cdot \mathbf{F}_A) = \frac{d\mathrm{k}_{AA}}{d\xi}, \tag{27}$$

where ξ is a parameter that uniquely represents the progress of the chemical reaction. The most common choice for ξ is the intrinsic reaction coordinate; however, it is not bound to any of the existing IRC computational schemes. Any predefined one-dimensional reaction path will do if only the external potential is uniquely defined by the reaction progress number ξ.[67] The derivative defined by Eq. (27) must be calculated for an atom exchanging electrons with the rest of the reacting system treated as a super-molecule. The electronic

population of an atom (N_A) varies with ξ. Thus, a bonded atom must be treated as an open system at the chemical potential equalized with the rest of the molecule.[44] For every step along the minimum-energy reaction coordinate, the rest of the system will be treated as an electron reservoir. The 1st order differential of k_{AA} can be formally written as

$$d\mathrm{k}_{AA} = \left(\frac{\partial \mathrm{k}_{AA}}{\partial \xi}\right)_{\mu} d\xi + \left(\frac{\partial \mathrm{k}_{AA}}{\partial \mu}\right)_{\xi} d\mu. \tag{28}$$

The atomic fragility is then directly related to the reaction electronic flux (J) parameter once identified by Toro-Labbé *et al.*[68,69] ($d\mu/d\xi = -J$),

$$a_{\xi}^{A} = \frac{d\mathrm{k}_{AA}}{d\xi} = \left(\frac{\partial \mathrm{k}_{AA}}{\partial \xi}\right)_{\mu} + \left(\frac{\partial \mathrm{k}_{AA}}{\partial \mu}\right)_{\xi} \frac{d\mu}{d\xi}. \tag{29}$$

The role of the other two derivatives must be elucidated. The first term can be expanded as

$$\left(\frac{\partial \mathrm{k}_{AA}}{\partial \xi}\right)_{\mu} = \sum_{B}^{atoms} \frac{d\mathbf{R}_B}{d\xi} \cdot [\nabla_B \mathrm{k}_{AA}]_{\mu}. \tag{30}$$

The derivative $[\nabla_B \mathrm{k}_{AA}]_{\mu}$ can be reduced to a simple form (for the proof, see Ref. 41)

$$[\nabla_B \mathrm{k}_{AA}]_{\mu} = [\nabla_B \mathrm{k}_{AA}]_{N} + S\boldsymbol{\Phi}_B \lambda_{AA} = \boldsymbol{a}_{BAA} + S\boldsymbol{\Phi}_B \lambda_{AA}. \tag{31}$$

Combining Eqs. (29) and (30) with the use of the definition of the nuclear reactivity $\boldsymbol{\Phi}_A$ [Eq. (8)] and reducing the resulting expansion lead to

$$\left(\frac{\partial \mathrm{k}_{AA}}{\partial \xi}\right)_{\mu} = \left(\frac{\partial \mathrm{k}_{AA}}{\partial \xi}\right)_{N} - \frac{d\mu}{d\xi} S\lambda_{AA}. \tag{32}$$

For the transformation of the second derivative needed in Eq. (29), the expression for the derivative $\widetilde{\lambda}_{AA}$ [supplementary material, Eq. S.(16)] will be useful,

$$\widetilde{\lambda}_{AA} = \left(\frac{\partial \widetilde{\mathrm{k}}_{AA}}{\partial \mu}\right)_{\xi} = S\lambda_{AA} + 2S^2 \boldsymbol{\Phi}_A \cdot \mathbf{G}_A + \gamma S^3 \boldsymbol{\Phi}_A^2. \tag{33}$$

Hence, using Eq. (14),

$$\left(\frac{\partial \mathrm{k}_{AA}}{\partial \mu}\right)_{\xi} = S\lambda_{AA} + 2S^2 \boldsymbol{\Phi}_A \cdot \mathbf{G}_A + \gamma S^3 \boldsymbol{\Phi}_A^2 + \left(\frac{\partial}{\partial \mu} S\boldsymbol{\Phi}_A^2\right)_{\xi}. \tag{34}$$

The formal expression for the atomic fragility [Eq. (29)] becomes

$$a_{\xi}^{A} = \left(\frac{\partial \mathrm{k}_{AA}}{\partial \xi}\right)_{N} + \left(2S^2 \boldsymbol{\Phi}_A \cdot \mathbf{G}_A + \gamma S^3 \boldsymbol{\Phi}_A^2\right) \frac{d\mu}{d\xi} + \frac{d}{d\xi}\left(S\boldsymbol{\Phi}_A^2\right). \tag{35}$$

k_{AA} needed in Eq. (35) will be taken from Eq. (24),

$$\mathrm{k}_{AA} = [\nabla_A \cdot \mathbf{F}_A]_N = 4\pi Z_A \rho(\mathbf{R}_A) + \iint s(\mathbf{r}, \mathbf{r}') \boldsymbol{\varepsilon}_A(\mathbf{r}') \cdot \boldsymbol{\varepsilon}_A(\mathbf{r}) d\mathbf{r} d\mathbf{r}' - S\boldsymbol{\Phi}_A^2. \tag{36}$$

Identifying the derivative $(\partial/\partial\xi)_N$ as $d/d\xi$ since N is a global variable, the basic formula for the peak intensity observed in atomic reaction fragility spectra is obtained as

$$a_{\xi}^{A} = 4\pi Z_A \frac{d}{d\xi}\rho(\mathbf{R}_A) + \frac{d}{d\xi}\left[\iint s(\mathbf{r}, \mathbf{r}') \boldsymbol{\varepsilon}_A(\mathbf{r}') \cdot \boldsymbol{\varepsilon}_A(\mathbf{r}) d\mathbf{r} d\mathbf{r}'\right] - JS^2 \boldsymbol{\Phi}_A \cdot (2\mathbf{G}_A + \gamma S \boldsymbol{\Phi}_A). \tag{37}$$

According to the maximum hardness principle discussed by Ordon and Tachibana,[47] $\mathbf{G}_A + \gamma S\boldsymbol{\Phi}_A = 0$, and the last term is reduced to $JS^2\boldsymbol{\Phi}_A \cdot \mathbf{G}_A$. Since the electric field derivative vanishes, as in Eq. (21), the integral in Eq. (37) (second term) is simplified even further. This is demonstrated using the expansion [as in Eq. (30)]

$$\frac{d\boldsymbol{\varepsilon}_A(\mathbf{r})}{d\xi} = \sum_{B}^{atoms} \frac{d\mathbf{R}_B}{d\xi} \cdot [\nabla_B \boldsymbol{\varepsilon}_A(\mathbf{r})]_N = 0. \tag{38}$$

The remaining integral in Eq. (37) will only contain one derivative $(ds(\mathbf{r}, \mathbf{r}')/d\xi)_N$. The local approximation successfully tested for the electric-field derivatives is helpful in reducing the result to a comprehensive level[70–72]

$$s(\mathbf{r}, \mathbf{r}') \cong s(\mathbf{r})\delta(\mathbf{r} - \mathbf{r}'). \tag{39}$$

The integral in Eq. (37) is then simplified to

$$\iint \frac{ds(\mathbf{r}, \mathbf{r}')}{d\xi} \boldsymbol{\varepsilon}_A(\mathbf{r}') \cdot \boldsymbol{\varepsilon}_A(\mathbf{r}) d\mathbf{r} d\mathbf{r}' = \int \frac{ds(\mathbf{r})}{d\xi} [\boldsymbol{\varepsilon}_A(\mathbf{r})]^2 d\mathbf{r}. \tag{40}$$

The amplitude of atomic peaks in the reaction fragility spectrum becomes

$$a_{\xi}^{A} = 4\pi Z_A \frac{d}{d\xi}\rho(\mathbf{R}_A) + \int \frac{ds(\mathbf{r})}{d\xi} [\boldsymbol{\varepsilon}_A(\mathbf{r})]^2 d\mathbf{r} - JS^2 \boldsymbol{\Phi}_A \cdot \mathbf{G}_A. \tag{41}$$

Equation (41) may be transformed even further by the electron-gas approximation in order to reveal the decisive factor that stimulates the reaction fragility spectrum intensity,

$$s(\mathbf{r}) = Sf(\mathbf{r}) = (S/N)\rho(\mathbf{r}) \qquad \text{(Refs. 10 and 7)}. \tag{42}$$

Finally, the relation of a_{ξ}^{A} to local-density changes induced by the ongoing reaction is

$$a_{\xi}^{A} = 4\pi Z_A \frac{d}{d\xi}\rho(\mathbf{R}_A) + \frac{S}{N} \int \frac{d\rho(\mathbf{r})}{d\xi} [\boldsymbol{\varepsilon}_A(\mathbf{r})]^2 d\mathbf{r} + A\frac{dS}{d\xi} - JS^2 \boldsymbol{\Phi}_A \cdot \mathbf{G}_A. \tag{43}$$

Here $A = (1/N) \int \rho(\mathbf{r}) [\boldsymbol{\varepsilon}_A(\mathbf{r})]^2 d\mathbf{r}$. The approximate expression [Eq. (43)] provides more understanding to the result [Eq. (41)] by exposing the nature of the terms contributing to the atomic fragility expression, a_{ξ}^{A}. The electron density at the nucleus $\rho(\mathbf{R}_A)$ should be weakly sensitive to the structural modification of the system introduced by the reaction (ξ) since only the valence electrons are responsible for the reaction. The second term in Eq. (43) appears to be the leading one, as it contains the integral strongly varying with the reaction progress (via $d\rho(\mathbf{r})/d\xi$) and localized on an atom. This makes it a local sensor for the electron density variations around one specific nucleus only. Substantial contributions to the integral in Eq. (43) come only from the areas where both the derivative $d\rho(\mathbf{r})/d\xi$ and the electric field of an atom $|\boldsymbol{\varepsilon}_A(\mathbf{r})|$ retain a

considerable value. This is the case of the creation or rupture of bonds by an atom.

The last two terms in Eq. (43) contain global parameters (J, S, and the integral A) also variable with $\rho(\xi)$ but are not related to $d\rho(\mathbf{r})/d\xi$. The effects of change in $\rho(\mathbf{r})$ are integrated over the whole system and the local variations are likely to be covered by the stable contributions from the parts of the system unperturbed by the reaction. This is also the case of two, seemingly local parameters, $\mathbf{\Phi}_A$, $\mathbf{G}_A$, defined by the integration [cf. Eqs. (8) and (10)] via the H—F force [Eq. (6)]. $S(\xi)$ dependence studied in earlier studies[47] showed merely a flat maximum near the TS.

The most significant feature of the above analysis is that it demonstrates the role of local factors in the observed atomic contribution to the reaction fragility a_ξ^A. It provides a tool to describe specifically an impact of the ongoing reaction on the electron density around a given atom, without predefining its range by any of the available arbitrary population-analysis algorithms. Discerning the effects introduced by the bonds around an atom is possible using the off-diagonal elements in the connectivity matrix. This has been demonstrated on the basis of numerical results for two standard reactions.

IV. RESULTS

The presented theoretical development of the fragility spectrum has been illustrated by simple numerical studies. For this purpose, we examined two test reactions involving different chemical transformations: the synthesis of HF + CO → HCOF and the isomerization of HONS→ONSH. The reactions are shown schematically in Schemes 1 and 2. IRC energy profiles were reproduced by the standard procedure at the MP2 level using the 6-311++G(*3df*,*3pd*) basis set and the Gaussian 09 code.[73] Our approach is not limited to any particular quantum chemical computational method; MP2 appears to be an optimal choice to obtain reliable (analytical) second derivatives. For larger systems, DFT methods would be more efficient due to reducing costs of calculations. Results given in Figs. 1 and 2 present the ξ-dependence of the $\underline{\underline{C}}$ matrix elements for both reactions. The energy diagrams for both systems have been published in earlier studies.[47,55] In Fig. 3 we present numerical results for the atomic fragility spectra obtained by taking numerical derivatives of the $k_{AA}(\xi)$ and $k_{AB}(\xi)$ functions vs. ξ. In both reactions, the meaningful variations of the connectivity matrix elements extend well beyond the hypothetical reaction region as limited by the minimum and maximum of the reaction force,[55] as indicated in the diagrams.

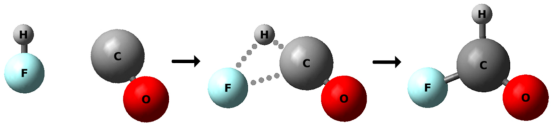

Reactant state (**RS**) Transition state (**TS**) Product state (**PS**)

SCHEME 1.

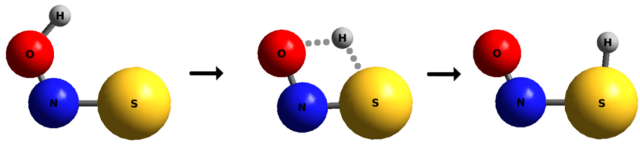

SCHEME 2.

Confronting Schemes 1 and 2 with the distribution of atomic peaks in the reaction fragility spectrum (Fig. 3) reveals the 1:1 correspondence between bond formation/rupture and the appearance of a pair of peaks for the two atoms affected. The evident examples are H—F, H—C and F—C bonds in Scheme 1 [Fig. 3(a)] and H—O and H—S bonds in Scheme 2 [Fig. 3(b)]. A more subtle modification of bonds is also visible in the O—C bond [Fig. 3(a)] and the O—N and N—S bonds [Fig. 3(b)]. Breaking the H—F bond is manifested by a strictly parallel decrease in k_{HH} and k_{FF} elements [Fig. 1(a)]. The next step of the reaction is also evident: formation of the C—H bond with parallel increase of k_{HH} and k_{CC} [Fig. 1(a)]. Very similar effects may be observed for the H—O and H—S bonds in Figs. 2(a) and 2(b). The peak intensities (areas) for atoms represent the charge flow to/from an atom by a rough relation[56] $\Delta k_{AA} = \overline{\lambda}_{AA} \cdot \Delta N_A$, where $\overline{\lambda}_{AA}$ stands for an average of the softening index over the peak region [Eq. (11)].

The striking similarity between atomic peaks in the spectra of atoms losing or forming a bond (as described above) provides a valuable justification for the role $d\rho(\mathbf{R}_A)/d\xi$ derivative in the final equation (43). If the contribution from the variable $\rho(\mathbf{R}_A)$ density alone were significant, it would have to introduce much different contributions for hydrogen and the atoms in the 2nd period as, e.g., fluorine. Apparently, it is the variable density in the valence region between atoms that provides a dominating contribution to the $a_\xi^A = dk_{AA}/d\xi$ derivative, at least for the two reactions studied in this work. The detailed resolution of other factors contributing to the atomic fragility [Eq. (43)] is open to further studies.

The intriguing feature of the reaction fragility spectra (Fig. 3) is that identification of atoms active in a bond modification is straightforward. Each broken bond appears as a pair of coupled downward peaks from the atomic contributions [e.g., H—F in Fig. 3(a) and (H)—(O) in Fig. 3(b)], while newly created bonds make pairs of the upwards peaks [e.g., H—C in Fig. 3(a) and (H)—(S) in Fig. 3(b)]. The exact reaction region (on the ξ axis) of bond modification is precisely reproduced, sometime quite late, as for the F—C bond in Fig. 3(a), that is only created beyond the range of any conceivable changes on the reaction path; this effect has been suggested earlier by the calculation of the Wiberg indices and the bond distance for the C—F bond.[55,56] The maximum of the fragility for C and F atoms is at $\xi \cong +3.4$, well away from the TS and very near to the energy minimum of products.

The atomic peaks on the fragility spectrum of the same atoms [Figs. 3(a) and 3(b)] are generally not transferable for different reactions except for the hydrogen atom. The hydrogen atom with poor electron density of its own makes a single bond only, and corresponding fragility peaks look alike for H—X bonds. This is not typical, as clearly seen for the oxygen atom in both systems under study. The oxygen atom in the HF/CO

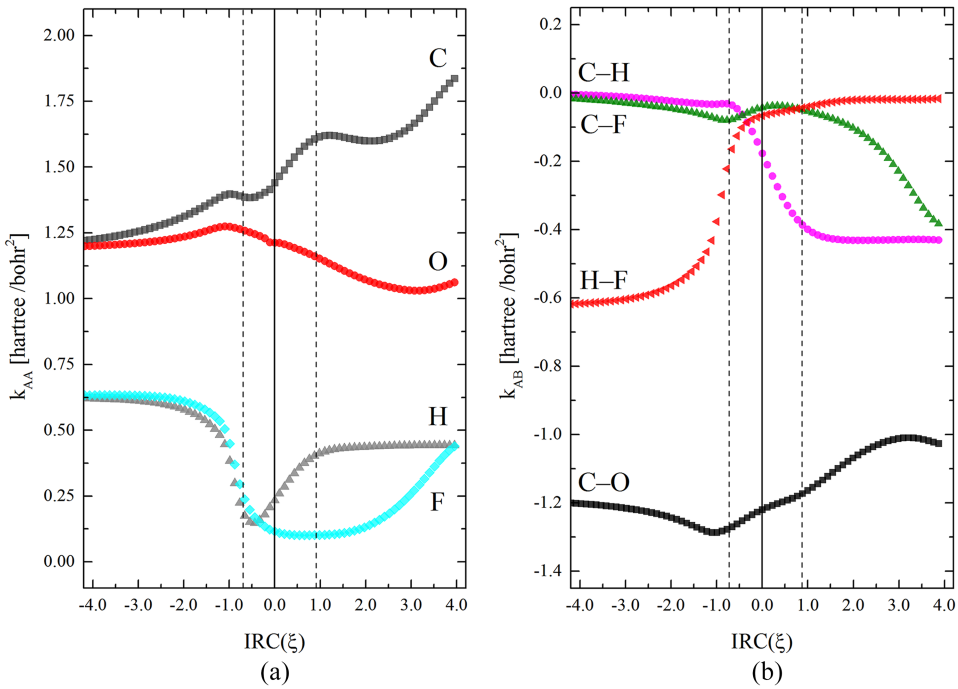

FIG. 1. Elements of the connectivity matrix (in a.u.) in the reaction[56] HF + CO → HCOF. (a) Diagonal elements. (b) Off-diagonal elements. Dashed lines indicate the hypothetical "reaction region" limited by the reaction-force extremes:[51] $dF_\xi/d\xi = 0$.

system does not change its formal bond but still shows a very broad fragility peak, mostly negative. This tends to indicate that by the attachment of H and F atoms to the central carbon, the C═O bond loses some density [Eq. (43)].

The off-diagonal elements resulting from Eq. (26) do not provide new global information since they sum up to the atomic contribution. The diagrams shown in Figs. 1(b) and 2(b) for the formal bonds generally parallel the diagrams of the Wiberg indices.[55] It is instructive to observe how the off-diagonal elements k_{AB} vary at crucial stages of the reaction; the data have been collected in Table I. Wherever a chemical bond does not exist, the k_{AB} elements are close to zero, as expected. When Eq. (24) is transformed using approximations in Eqs. (39) and (42), the off-diagonal elements of the connectivity matrix become

$$[\nabla_A \cdot \mathbf{F}_B]_N = -S\mathbf{\Phi}_A \cdot \mathbf{\Phi}_B + \frac{S}{N}\int \rho(\mathbf{r})\boldsymbol{\varepsilon}_A(\mathbf{r}) \cdot \boldsymbol{\varepsilon}_B(\mathbf{r})d\mathbf{r}. \qquad (44)$$

The value of the integral in Eq. (44) is determined by two factors: electric density $\rho(\mathbf{r})$ and the scalar product of two electric field vectors originated from two nuclei A and B of atoms at a distance. For non-bonded atoms, the classical ESF-(conceptual) electrostatic force analysis by Nakatsuji is helpful in clarifying the panorama of acting forces: the atomic dipole force (AD), the exchange force (EC), and

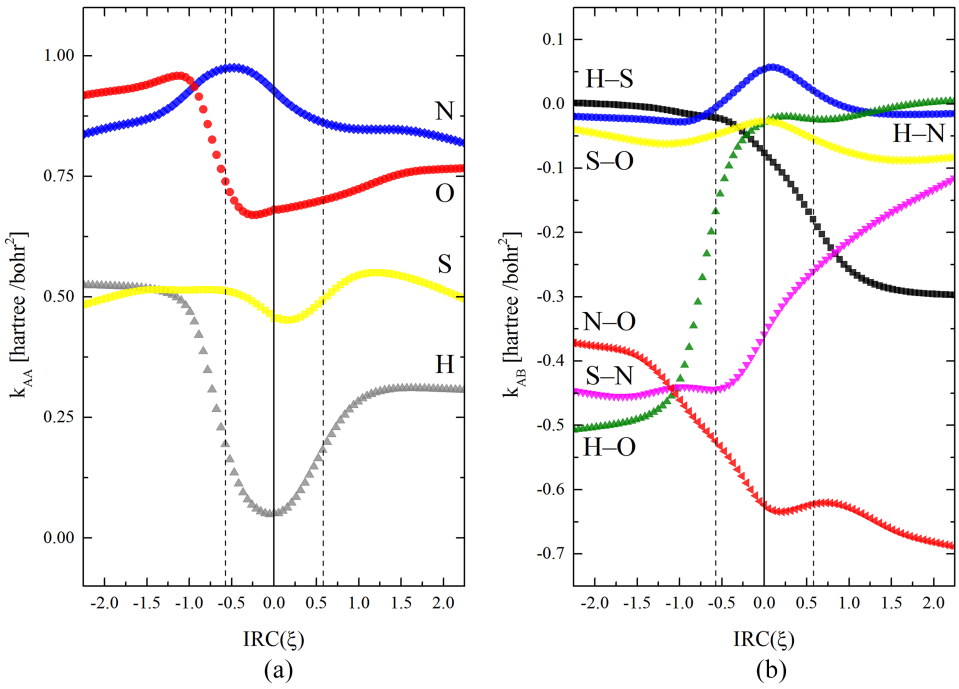

FIG. 2. Elements of the connectivity matrix (in a.u.) in the reaction:[56] HONS → ONSH. (a) Diagonal elements. (b) Off-diagonal elements. Dashed lines indicate the hypothetical "reaction region" limited by the reaction force extremes:[51] $dF_\xi/d\xi = 0$.

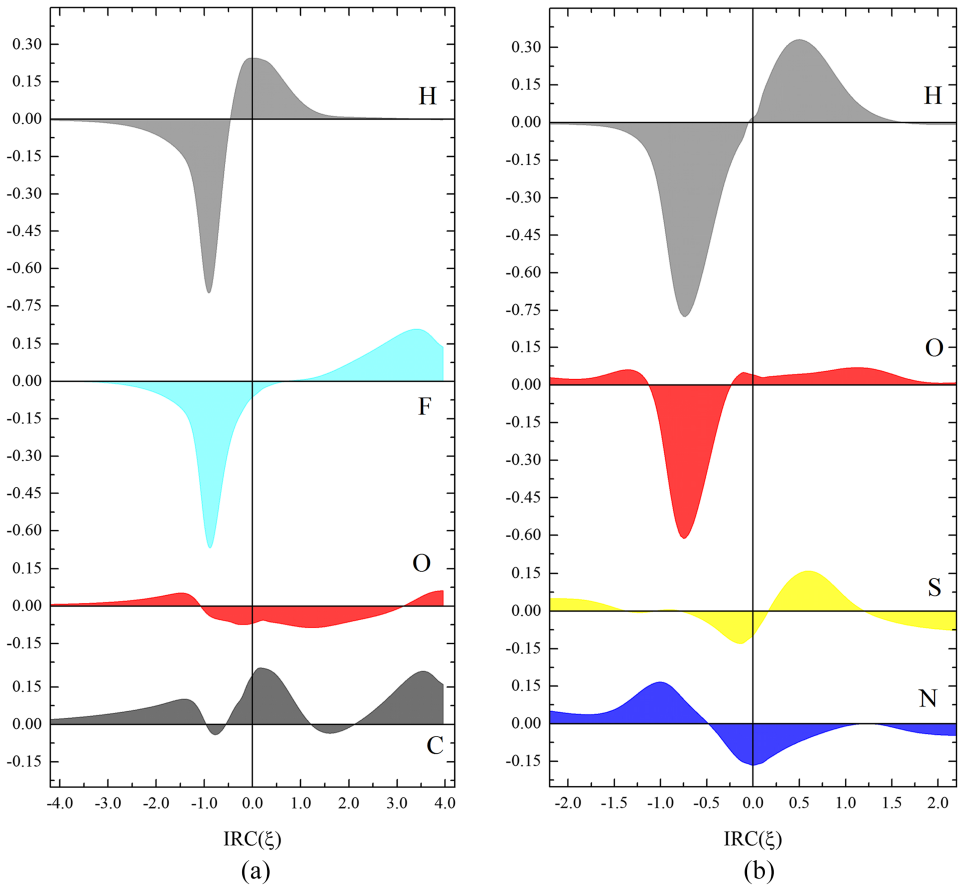

FIG. 3. Atomic reaction fragility spectra; the derivative $a^A_\xi = \frac{d}{d\xi}(\nabla_A \cdot \mathbf{F}_A)$ is given on the ordinate axis (atomic units). (a) HF + CO → HCOF; (b) HONS → ONSH.

the gross charge force (GC).[74] The integral in Eq. (44) is negligible for various reasons for each type of force. The EC force vanishes wherever there is no bond density. Contributions from AD and GC forces are small since $\boldsymbol{\varepsilon}_A(\mathbf{r}) \cdot \boldsymbol{\varepsilon}_B(\mathbf{r})$ terms cancel out when integrated with nearly symmetrical core density at A and B that is dominating in the integral. Only deviations of the spherical density distribution in the vicinity of both atoms contribute to $\nabla_A \cdot \mathbf{F}_B$. The leftover values in Table I for non-bonded atoms (as opposed to those for bonded pairs) are likely to represent the product $S\boldsymbol{\Phi}_A \cdot \boldsymbol{\Phi}_B$ only.

TABLE I. Off-diagonal elements of the connectivity matrix [k_{AB} Eq. (24)] calculated for the reactant state (RS), transition state (TS), and product state (PS) in the reactions HF/CO and H/ONS (in a.u.). The existence of formal bonds has been indicated by shadowing.

	HF + CO → HCOF (Scheme 1)					
Bond	C—O	C—H	C—F	O—H	O—F	H—F
RS($\xi = -4$)	−1.20	−0.01	−0.02	0.00	0.00	−0.62
TS($\xi = 0$)	−1.21	−0.21	−0.04	0.01	−0.01	−0.06
PS($\xi = 4$)	−1.03	−0.43	−0.38	0.00	−0.04	−0.02
	HONS → ONSH (Scheme 2)					
Bond	N—O	N—H	N—S	S—H	S—O	H—O
RS($\xi = -2$)	−0.38	−0.02	−0.45	0.00	−0.05	−0.50
TS($\xi = 0$)	−0.63	0.06	−0.35	−0.08	−0.03	−0.02
PS($\xi = 2$)	−0.68	−0.02	−0.13	−0.30	−0.09	0.00

It is informative to compare the k_{AB} elements for the bonds formed by a central atom with a group of its neighbors. By selecting an observation point on C and N for both systems, respectively, it is shown that the off-diagonal elements of $\underline{\underline{C}}$ matrix provide a reasonable measure for the relative strength of the respective bonds around a central atom (Table I),

$$k_{CO}(RS) : k_{CO}(PS) \cong 1.2 : 1,$$
$$k_{CO}(PS) : k_{CH}(PS) : k_{CF}(PS) \cong 2.7 : 1.1 : 1,$$
$$k_{NO}(RS) : k_{NO}(PS) \cong 1 : 1.8,$$
$$k_{NS}(RS) : k_{NS}(PS) \cong 3.5 : 1,$$
$$k_{NO}(RS) : k_{OH}(RS) : k_{NS}(RS) \cong 1 : 1.3 : 1.2,$$
$$k_{NO}(PS) : k_{SH}(PS) : k_{NS}(PS) \cong 2.3 : 1 : 0.4.$$

The difference between the C—O bond in a free CO molecule and in the HCOF entity is notable, as is the similarity between the H—C and C—F bonds. According to the bond k_{AB} ratio in the H—O—N=S molecule, all three bonds are of similar strength, although N=S is formally a double bond. Transformation to O=N—S—H is marked by doubling the N=O strengths and the decrease of the N—S bond to less than $^1/_3$ of the initial value, making it, very realistically, the weakest point of the product molecule.

Another valuable observation in Table I is the uniquely positive value of the k_{NH} element in the transition state (TS) of the H/ONS system, also observed as a maximum in Fig. 2(b). The distortions from spherical symmetry around the moving proton are unquestionable and this makes the integral equation (44) large as for a non-bonded pair. This is in harmony

with the old suggestion by Parr that deviations of symmetry in the density occur only in the immediate vicinities of atoms when they are bonded.[75] This effect marks an unstable point on the reaction path that is uniquely responsible for the TS, unlike the HF/CO reaction where the formal TS marked by the energy maximum does not show structural instabilities. This insight into the role of structural changes upon a reaction is new and is a very valuable feature of this present analysis.

V. DISCUSSION AND CONCLUSION

Judging the role of terms in the working final equation [Eq. (43)] is possible by studying the effect of twin atomic peaks on the atomic fragility spectra for bonded atoms. The only term that is likely to equally contribute to a_ξ^A of both partners is the density change in a bond making an element common for both $d\rho(\mathbf{r})/d\xi$. The effect is strictly localized on the reaction path for some atoms well beyond the TS [e.g., the C—F bond, Fig. 3(a)]. The role of the last term in Eq. (43) $JS^2\mathbf{\Phi}_A \cdot \mathbf{G}_A$ must also be considered. An estimation of the magnitude of that term is possible using the values reported in the literature for its components. The combined effect is dominated by the small value of J (up to ca. ±200 kcal/mol≅ ±0.03 a.u.[68,69]) and $|\mathbf{\Phi}_A|, |\mathbf{G}_A|$ (ca. 0.02–0.2 a.u.[33]). Including the softness factor ($S^2 \cong 1 \div 10$ a.u.[47]), the $JS^2\mathbf{\Phi}_A \cdot \mathbf{G}_A$ term may be smaller than 1% of the fragility peaks intensity, ca. 0.1–1 a.u.; the leading term in Eq. (43) is most likely the one reporting the variation of electronic density due to the bond formation of breaking.

The crucial result of this work is the connectivity matrix, resulting from the formulation of the second-energy derivatives over atomic displacements (cumulative force constants) as divergences of the Hellmann-Feynman forces, rather than derivatives over the coordinates. This produces a significant consequence: the divergences are invariants, either focused on atoms or on the bonds; moreover, they do not contain the nuclear-repulsion energy component. The overall trace of the Hessian is now decomposed into pure atomic contributions (k_{AA}), which is an alternative to the Wilson method of dividing it into the contributions from the normal modes.[76,77] This difference is of great advantage in monitoring a system undergoing a reaction. The variable atomic contributions to the connectivity matrix reflect strengthening or loosening of actual bonds upon a reaction in the framework of the Born-Oppenheimer approximation.

Other principal outcomes of this work are the following: (i) Definition of the atomic fragility as the derivative over the reaction progress ξ of the Hellman-Feynman force divergence for an atom (the diagonal elements of the connectivity matrix). (ii) Proving the approximate relation between the atomic fragility on a reaction path and the electron density changes in the bond region of an atom, with only minor contribution from the global effects [Eq. (43)]. (iii) Demonstrating that the atomic fragility spectrum tends to indicate the bonds created or broken in a reaction and appears to be dominated by the electron density variation in the bonds for the investigated example reactions. Although the fragility spectrum is focused on an atom, no formal definition for an-atom-in-molecule is necessary for the analysis. (iv) The off-diagonal terms of the connectivity matrix provide a precise classification of the actual bonds formed by an atom with any of its neighbors.

SUPPLEMENTARY MATERIAL

See supplementary material for the details concerning the notation and calculation of the electrostatic potential divergences and the expressions for the derivatives of the grand potential in the nuclear coordinate representation for an open system. References to this material have been marked in the main text.

ACKNOWLEDGMENTS

The authors dedicate their work to the memory of Professor Józef Lipiński (1948-2016), their long-time coworker, co-author, and friend.

The authors are gratefully indebted to Professor Craig J. Eckhardt (Department of Chemistry, University of Nebraska–Lincoln, USA) for critically reading the manuscript and many enlightening remarks.

This work was financed by a statutory activity subsidy from the Polish Ministry of Science and Higher Education for the Faculty of Chemistry of the Wrocław University of Science and Technology, Ref. No. 0401/0257/16. Calculations have been carried out using resources provided by Wroclaw Centre for Networking and Supercomputing (http://wcss.pl), Grant Nos. 249 and 236.

[1] R. G. Parr and W. Yang, J. Am. Chem. Soc. **106**, 4049 (1984).
[2] K. Fukui, Acc. Chem. Res. **14**, 363 (1981).
[3] R. G. Parr, R. A. Donelly, M. Levy, and W. E. Palke, J. Chem. Phys. **68**, 3801 (1978).
[4] R. G. Parr and R. G. Pearson, J. Am. Chem. Soc. **105**, 7512 (1983).
[5] H. Chermette, J. Comput. Chem. **20**, 129 (1999).
[6] P. Geerlings and F. De Proft, Phys. Chem. Chem. Phys. **10**, 3028 (2008).
[7] P. Geerlings, F. De Proft, and W. Langenaeker, Chem. Rev. **103**, 1793 (2003).
[8] P. W. Ayers and R. G. Parr, J. Am. Chem. Soc. **123**, 2007 (2001).
[9] R. F. Nalewajski, Adv. Quantum Chem. **51**, 235 (2006).
[10] P. W. Ayers and R. G. Parr, J. Am. Chem. Soc. **122**, 2010 (2000).
[11] R. G. Parr and W. Yang, *Density Functional Theory of Atoms and Molecules* (Oxford University Press, Oxford, UK, 1989).
[12] R. F. Nalewajski and R. G. Parr, J. Chem. Phys. **77**, 399 (1982).
[13] R. F. Nalewajski, J. Chem. Phys. **81**, 2088 (1984).
[14] R. F. Nalewajski, J. Chem. Phys. **78**, 6112 (1983).
[15] R. F. Nalewajski, Z. Naturforsch. **43**, 65 (1988).
[16] R. F. Nalewajski and J. Korchowiec, J. Mol. Catal. **54**, 324 (1989).
[17] R. F. Nalewajski and J. Mrozek, Int. J. Quantum Chem. **43**, 353 (1992).
[18] A. Michalak, M. Mitoraj, and T. Ziegler, J. Phys. Chem. A **112**, 1933 (2008).
[19] M. P. Mitoraj, A. Michalak, and T. Ziegler, J. Chem. Theory Comput. **5**, 962 (2009).
[20] M. P. Mitoraj, M. Parafiniuk, M. Srebro, M. Handzlik, A. Buczek, and A. Michalak, J. Mol. Model. **17**, 2337 (2011).
[21] P. W. Ayers and R. G. Parr, J. Chem. Phys. **129**, 054111 (2008).
[22] C. Cárdenas, E. Echegaray, D. Chakraborty, J. S. M. Anderson, and P. W. Ayers, J. Chem. Phys. **130**, 244105 (2009).
[23] P.-H. Liu and K. L. C. Hunt, J. Chem. Phys. **103**, 10597 (1995).
[24] K. L. C. Hunt, J. Chem. Phys. **103**, 3552 (1995).
[25] E. L. Tisko and K. L. C. Hunt, J. Chem. Phys. **103**, 6873 (1995).
[26] K. L. C. Hunt, J. Chem. Phys. **90**, 4909 (1989).
[27] R. P. Feynman, Phys. Rev. **56**, 340 (1939).
[28] K. L. C. Hunt and Y. Q. Liang, J. Chem. Phys. **95**, 2549 (1991).

[29]M. H. Cohen, M. V. Ganduglia-Pirovano, and J. Kudrnovsky, J. Chem. Phys. **101**, 8988 (1994).
[30]B. G. Baekelandt, A. Cedillo, and R. G. Parr, J. Chem. Phys. **103**, 8548 (1995).
[31]M. Berkowitz, S. K. Ghosh, and R. G. Parr, J. Am. Chem. Soc. **107**, 6811 (1985).
[32]B. G. Baekelandt, J. Chem. Phys. **105**, 4664 (1996).
[33]P. Ordon and L. Komorowski, Chem. Phys. Lett. **292**, 22 (1998).
[34]F. De Proft, S. Liu, and P. Geerlings, J. Chem. Phys. **108**, 7549 (1998).
[35]L. Komorowski and P. Ordon, Theor. Chem. Acc. **105**, 338 (2001).
[36]R. Balawender and P. Geerlings, J. Chem. Phys. **114**, 682 (2001).
[37]L. Komorowski and P. Ordon, J. Mol. Struct.: THEOCHEM **630**, 25 (2003).
[38]L. Komorowski and P. Ordon, Int. J. Quantum Chem. **91**, 398 (2003).
[39]P. Ordon and L. Komorowski, Int. J. Quantum Chem. **101**, 703 (2005).
[40]T. Luty, P. Ordon, and C. J. Eckhardt, J. Chem. Phys. **117**, 1775 (2002).
[41]L. Komorowski and P. Ordon, Int. J. Quantum Chem. **99**, 153 (2004).
[42]H. Nakatsuji, J. Am. Chem. Soc. **96**, 30 (1974).
[43]W. H. Miller, N. C. Handy, and J. E. Adams, J. Chem. Phys. **72**, 99 (1980).
[44]R. F. Nalewajski, Phys. Chem. Chem. Phys. **1**, 1037 (1999).
[45]J. G. Lopez, G. Vayner, U. Lourderaj, S. V. Addepalli, S. Kato, W. A. deJong, T. Windus, and W. L. Hase, J. Am. Chem. Soc. **129**, 9976 (2007).
[46]P. Hohenberg and W. Kohn, Phys. Rev. **136**, B864 (1964).
[47]P. Ordon and A. Tachibana, J. Chem. Phys. **126**, 234115 (2007).
[48]A. Toro-Labbé, J. Phys. Chem. A **103**, 4398 (1999).
[49]J. Martinez and A. Toro-Labbé, J. Math. Chem. **45**, 911 (2009).
[50]P. Politzer, A. Toro-Labbé, S. Gutiérrez-Oliva, and J. S. Murray, "Perspectives on the reaction force," in *Perspectives on the Reaction Force in Advances in Quantum Chemistry*, edited by J. R. Sabin and E. J. Brändas (Elsevier, Amsterdam, 2012), Vol. 64, pp. 189–210.
[51]A. Toro-Labbé, S. Gutiérrez-Oliva, P. Politzer, and J. S. Murray, "Reaction force: A rigorously defined approach to analyzing chemical and physical processes," in *Chemical Reactivity Theory. A Density Functional Viewpoint*, edited by P. K. Chattaraj (CRC Press, Taylor & Francis Group, Boca Raton, USA, 2009), pp. 293–302.
[52]P. Ordon and A. Tachibana, J. Mol. Model. **11**, 312 (2005).
[53]P. Ordon and A. Tachibana, J. Chem. Sci. **117**, 583 (2005).
[54]C. A. Gonzalez, E. Squitieri, H. J. Franco, and L. C. Rincon, J. Phys. Chem. A **121**, 648 (2017).
[55]M. Jędrzejewski, P. Ordon, and L. Komorowski, J. Phys. Chem. A **120**, 3780 (2016).
[56]L. Komorowski, P. Ordon, and M. Jędrzejewski, Phys. Chem. Chem. Phys. **18**, 32658 (2016).
[57]S. J. Klippenstein, V. S. Pande, and D. G. Truhlar, J. Am. Chem. Soc. **136**, 528 (2014).
[58]S. Beegum, Y. S. Mary, H. T. Varghese, C. Y. Panicker, S. Armaković, S. J. Armaković, J. Zitko, M. Dolezal, and C. Van Alsenoy, J. Mol. Struct. **1131**, 1 (2017).
[59]S. Pratihar, X. Ma, Z. Homayoon, G. L. Barnes, and W. L. Hase, J. Am. Chem. Soc. **139**, 3570 (2017).
[60]R. Sun, K. Park, W.A. de Jong, H. Lischka, T. L. Windus, and W. L. Hase, J. Chem. Phys. **137**, 044305 (2012).
[61]P. W. Ayers, J. S. M. Anderson, and L. Bartolotti, Int. J. Quantum Chem. **101**, 520 (2005).
[62]P. Ordon, Ph.D. thesis, Wrocław University of Technology, 2003.
[63]M. Berkowitz and R. G. Parr, J. Chem. Phys. **88**, 2554 (1988).
[64]L. Salem, J. Chem. Phys. **38**, 1227 (1963).
[65]L. Salem and M. Alexander, J. Chem. Phys. **39**, 2994 (1963).
[66]L. Salem and E. B. Wilson, Jr., J. Chem. Phys. **36**, 3421 (1962).
[67]A. Tachibana and R. G. Parr, Int. J. Quantum Chem. **41**, 527 (1992).
[68]E. Echegeray and A. Torro-Labbé, J. Phys. Chem. A **112**, 11801 (2008).
[69]J. I. Martínez-Araya and A. Toro-Labbé, J. Phys. Chem. C **119**, 3040 (2015).
[70]A. Vela and J. L. Gazquez, J. Am. Chem. Soc. **112**, 1490 (1990).
[71]L. Komorowski, J. Lipiński, and P. Szarek, J. Chem. Phys. **131**, 124120 (2009).
[72]L. Komorowski, J. Lipiński, P. Szarek, and P. Ordon, J. Chem. Phys. **135**, 014109 (2011).
[73]M. J. Frisch, G. W. Trucks, H. B. Schlegel, G. E. Scuseria, M. A. Robb, J. R. Cheeseman, J. A. Montgomery, Jr., T. Vreven, K. N. Kudin, J. C. Burant, J. M. Millam, S. S. Iyengar, J. Tomasi, V. Barone, B. Mennucci, M. Cossi, G. Scalmani, N. Rega, G. A. Petersson, H. Nakatsuji, M. Hada, M. Ehara, K. Toyota, R. Fukuda, J. Hasegawa, M. Ishida, T. Nakajima, Y. Honda, O. Kitao, H. Nakai, M. Klene, X. Li, J. E. Knox, H. P. Hratchian, J. B. Cross, C. Adamo, J. Jaramillo, R. Gomperts, R. E. Stratmann, O. Yazyev, A. J. Austin, R. Cammi, C. Pomelli, J. W. Ochterski, P. Y. Ayala, K. Morokuma, G. A. Voth, P. Salvador, J. J. Dannenberg, V. G. Zakrzewski, S. Dapprich, A. D. Daniels, M. C. Strain, O. Farkas, D. K. Malick, A. D. Rabuck, K. Raghavachari, J. B. Foresman, J. V. Ortiz, Q. Cui, A. G. Baboul, S. Clifford, J. Cioslowski, B. B. Stefanov, G. Liu, A. Liashenko, P. Piskorz, I. Komaromi, R. L. Martin, D. J. Fox, T. Keith, M. A. Al-Laham, C. Y. Peng, A. Nanayakkara, M. Challacombe, P. M. W. Gill, B. Johnson, W. Chen, M. W. Wong, C. Gonzalez, and J. A. Pople, GAUSSIAN 09, Revision A.02, Gaussian, Inc., Wallingford, CT, 2009.
[74]H. Nakatsuji, J. Am. Chem. Soc. **95**, 345 (1973).
[75]R. G. Parr, J. Chem. Phys. **40**, 3726 (1964).
[76]E. B. Wilson, Jr., J. C. Decius, and P. C. Cross, *Molecular Vibrations* (Dover Publications, New York, USA, 1980).
[77]S. J. Cyvin, *Molecular Vibrations and Mean Square Amplitudes* (Elsevier, Amsterdam, 1968).